Thermal Wetting of Platinum Nanocrystals on Silica Surface

Rong Yu,[†] Hyunjoon Song,[†,‡,§] Xiao-Feng Zhang,[†] and Peidong Yang*,[†,‡]

Materials Sciences Division, Lawrence Berkeley National Laboratory, Berkeley, California 94720, and Department of Chemistry, University of California, Berkeley, California 94720

Received: February 24, 2005; In Final Form: March 20, 2005

Thermal stability of facetted Pt nanocrystals on amorphous silica support films was investigated using in situ transmission electron microscopy in a temperature range between 25 and 800 °C. The particles started to change their shapes at ∼350 °C. Above 500 °C, the particles spread on the support film with increasing temperature, rather than becoming more spherical. Such temperature-induced wetting of Pt nanoparticles on silica surface can be attributed to the interfacial mixing of Pt and SiO_2 and the resulting negative interface energy.

For heterogeneous catalysis, both metal and metal−support interactions are crucial in determining catalytic properties.[1−4] In particular, the thermal stability and shape evolution of active metal nanoparticles supported on different substrates at elevated temperatures need to be studied carefullly,[5−9] as many practical catalytic reactions utilized in industry take place at high temperatures.

It is a general tendency that the metal particles become spherical-like at high temperatures to lower the total surface area and the surface energy.[10,11] Recently, Wang et al. reported a temperature-dependent shape transformation of the Pt nanoparticles on an amorphous carbon substrate. They showed that the particles were transformed into a spherical-like shape by surface melting and eventually agglomerated at high temperatures.[5] However, in the present study, we observed by using in situ transmission electron microscopy (TEM) that the Pt nanoparticles spread on the amorphous SiO_2 substrates at temperatures above 500 °C. It indicates that for Pt nanoparticles on SiO_2, a typical heterogeneous catalyst, Pt tends to wet the SiO_2 surface instead of forming spherical particles.

Two different shapes of Pt nanoparticles (samples A and B) were produced by modified polyol process in the presence of poly(vinylpyrrolidone) (PVP).[12] Briefly, 2.5 mL of ethylene glycol (EG) was refluxed for 5 min. A total of 0.5 mL of $AgNO_3$ solution was added to the boiling EG. Immediately, EG solutions of PVP (93.8 μL, 0.375 M) and $H_2PtCl_6\cdot6H_2O$ (46.9 μL, 0.0625 M) were added to the mixture every 30 s over a 16-min period. The resulting solution was refluxed for an additional 5 min. For samples A and B, 2×10^{-3} M (Ag/Pt = 1.1 mol %) and 2×10^{-2} M (Ag/Pt = 11 mol %) of $AgNO_3$ stock solutions in EG were used, respectively. The products were purified by repetitive precipitation and centrifugation and finally dispersed in ethanol. The TEM samples were prepared by dropping specimen solution on copper grids with amorphous silica films

(Structure Probe, Inc.). Sample A consisted of 80% Pt cubes (average vertex-to-vertex distance: 9.4 ± 0.6 nm) and 10% of Pt tetrahedra (9.8 ± 0.7 nm). Sample B was dominated by Pt cuboctahedra (9.1 ± 0.6 nm), measured by TEM at room temperature.[12]

The in situ heating experiments were carried out using a JEOL JEM-3010 transmission electron microscope, operating at 300 kV. The microscope employs a LaB_6 thermal emission gun. The vacuum in the column is about 3×10^{-6} Pa. The specimens were heated slowly from room temperature to 800 °C in 6−7 h to get the systems close to equilibrium. The temperature was measured using a thermocouple attached to the specimen cup. The analyzed areas were selected to be close to the Cu grid to minimize the temperature difference between the specimen cup and the sample areas.

The shape of the particles at room temperature was characterized.[12] The cubic particles were enclosed by six {100} planes, of which the 12 edges were along ⟨100⟩ directions. The tetrahedral particles were enclosed by four {111} faces, and the six edges were along ⟨110⟩ directions. The cuboctahedral (also known as "truncated octahedral") particles were enclosed by both {111} and {110} planes, with edges lying in ⟨100⟩ and ⟨110⟩ directions.

Figure 1, parts a and b, shows the in situ TEM images of samples A and B, respectively. For the particles with cubic and tetrahedral shapes (Figure 1a), the truncation started to develop at ∼350 °C, consistent with the previous results of Pt nanoparticles on a carbon support by Wang et al.[5] When the temperature increased to 550 °C, the shape of the particles was hardly identifiable between cubes and tetrahedra due to significant truncation. The particles became irregularly faceted at higher temperatures. In a few cases, the directions of the edges were derived from the relative orientations of the particles at high and low temperatures. For example, some tetrahedral particles possess a truncated rectangular shape at high temperatures, two of which are indicated by arrows in the snapshot taken at 800 °C. As schematically shown in Figure 1c, the short edges of the rectangles are parallel to the edges of the tetrahedral particles at low temperatures, which lie in ⟨110⟩ directions. The

---

* Corresponding author. E-mail: p_yang@berkeley.edu.
[†] Lawrence Berkeley National Laboratory.
[‡] University of California, Berkeley.
[§] Current address: Department of Chemistry, Korea Advanced Institute of Science and Technology, Daejeon, 305-701 Korea.

Letters

J. Phys. Chem. B, Vol. 109, No. 15, 2005 **6941**
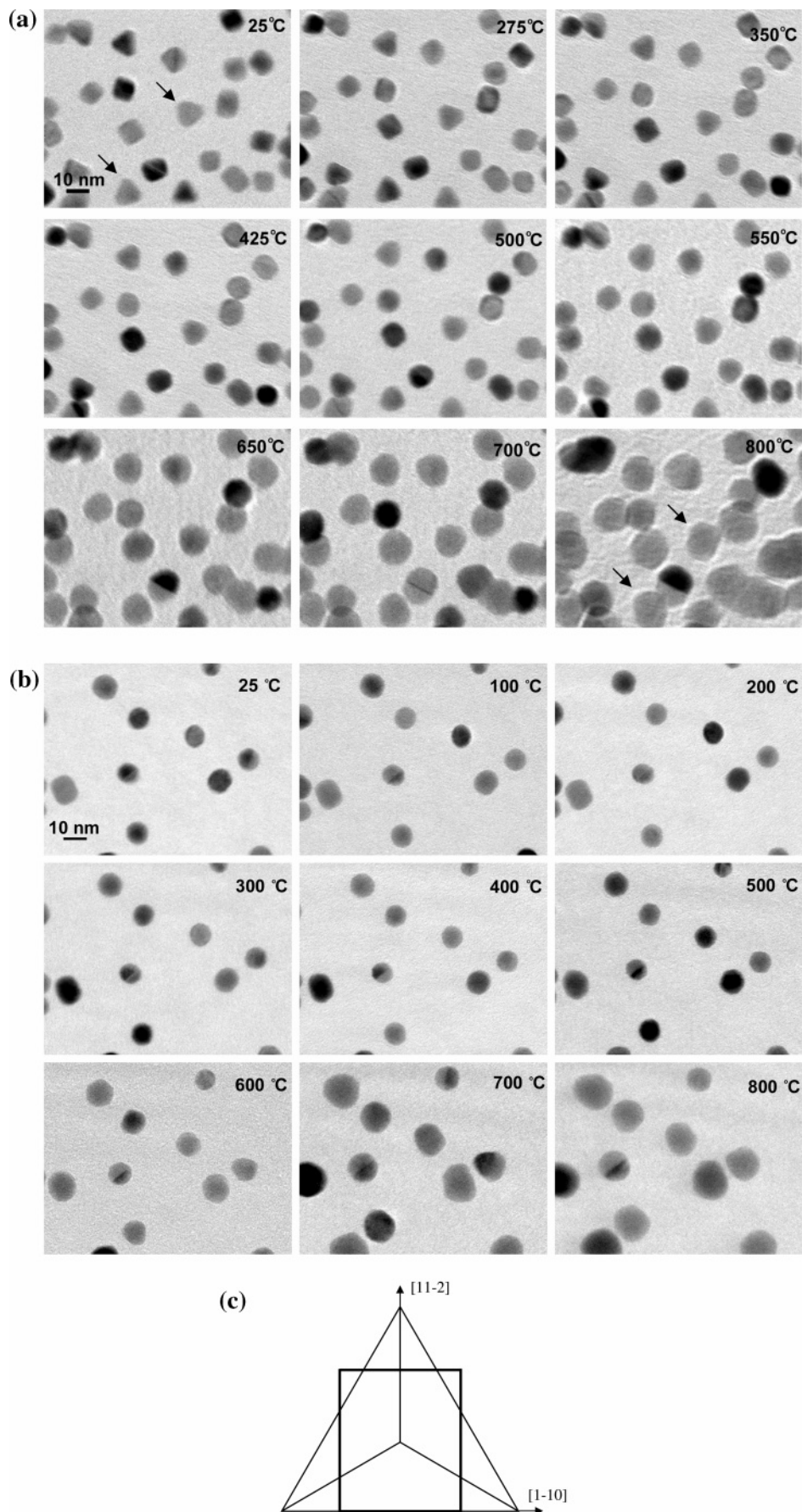
Figure 1. In situ TEM images of the Pt nanoparticles recorded during the heating process, showing the temperature-induced change of shape and wetting of Pt on silica. (a) Mixed cubic and tetrahedral particles from sample A. (B) Cuboctahedral particles from sample B. Two tetrahedral particles transformed to truncated rectangular shapes at high temperatures are indicated by arrows in (a) and schematically shown in (c).
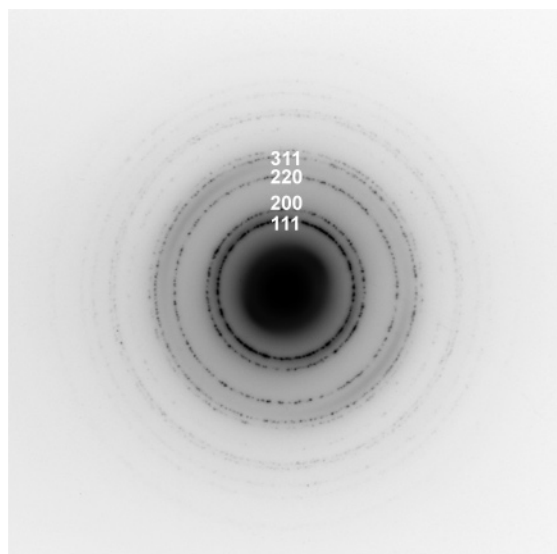
Figure 2. Selected-area electron diffraction pattern of the Pt nanoparticles on amorphous SiO_2 substrate (sample A) taken at 725 °C, indicating no secondary phases at high temperatures. The indices are for Pt crystal lattice.

long edges are perpendicular to the short edges; they lie in ⟨112⟩ directions. As a comparison, we have also carried out the ex situ heating experiments. The Pt nanocubes were heated on silica grids under oxygen flow. After thermal treatment at 300 °C for 6 h, most of the particles still maintained their original shapes, although particle aggregation was observed under such conditions.

Because the cuboctahedral particles were truncated even at room temperature, the shape change (Figure 1b) was not as obvious as those of the cubic and tetrahedral particles. At room temperature, they were enclosed by small facets and looked like spheres. Similar to the cubic and the tetrahedral particles, the cuboctahedral particle shape was converted to irregular ones at higher temperatures.

Some particles shown in Figure 1, parts a and b, are bicrystals. There is no change in the length of the grain boundaries with increasing temperature (i.e., they extend to surfaces even at 800 °C), which suggests that surface melting did not occur for these Pt nanoparticles. It is also noted that no secondary phases such as platinum silicide formed at high temperatures. Figure 2 shows a selected-area electron diffraction pattern of sample A taken at 725 °C, exhibiting the sharp spots/rings only from metal Pt. This is in contrast to the reports[6−8] that platinum silicides formed in Pt−SiO_2 systems. The reason for the difference is believed to be the treatment of the samples in reducing H_2 ambient for the latter cases.

The thermal stability of the polymer (PVP) layer enclosing the Pt nanoparticles is not available in the present study, mainly because the layer did not generate enough contrast from the SiO_2 substrate. It was demonstrated that, however, the polymer layer can be completely removed below 250 °C in the high vacuum environment of the TEM column.[5] In ref 5, Pt particles attached at the edge of the grid were investigated using a TEM with a cold-field-emission gun, which generates a higher coherent electron beam than a thermal emission gun and thus higher contrast for the polymer layer.

Metal particles usually become more spherical-like at high temperatures to lower the surface energy.[10,11] Thus, in TEM images, the projection area of the particles is expected to decrease with increasing temperature.[5] However, in the present study, the projection areas increased with rising temperature as
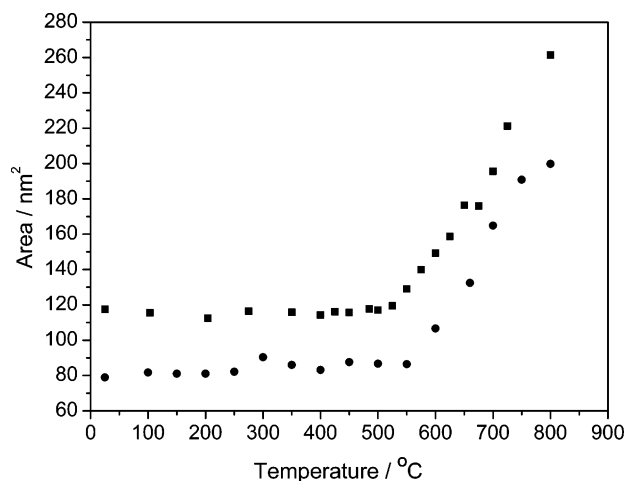
Figure 3. Projection area of Pt nanoparticles on silica support as a function of temperature, showing a critical temperature of around 500 °C, above which the particles spread (wetting) on the SiO_2 support films. The squares and circles represent data from samples A and B, respectively.

shown in, parts a and b of Figure 1. Statistical mean projection area of the particles is plotted against the temperature change in Figure 3. A critical temperature T_C around 500 °C is clearly observed, and the projection area (or the Pt/SiO_2 interface) below T_C remains almost constant with increasing temperature. Above T_C, the interface area increases rapidly with the increase of temperature. In the following, we will show that this temperature-induced wetting of Pt on SiO_2 can be attributed to the interfacial mixing and the negative interface energy.

Because the investigated particles were faceted at high temperatures, there was more than one contact angle between the particles and the substrates, and the accurate values were not generally available. However, by assuming a constant volume and spherical surface for the particles, the average contact angle can be estimated from the projection area (see the Supporting Information for details). Then the interface energy is obtained using the Young−Dupre equation[11]

$$\gamma_{int} = \gamma_{SiO_2} - \gamma_{Pt} \cos \theta \qquad (1)$$

where γ_{int} denotes the interface energy between Pt and SiO_2, γ_{SiO_2} is the surface energy of SiO_2, γ_{Pt} is the surface energy of Pt, and θ is the contact angle. The work of adhesion is calculated using

$$W_{ad} = \gamma_{Pt} + \gamma_{SiO_2} - \gamma_{int} = \gamma_{Pt} (1 + \cos \theta) \qquad (2)$$

The surface energies of Pt and SiO_2 are required in eqs 1 and 2. γ_{Pt} is 2.2 N/m at 1300 °C with a temperature coefficient of −0.60 mN/mK;[11] γ_{SiO_2} is 0.278 N/m at 1000 °C with a temperature coefficient of 0.035 mN/mK.[13] The Pt/SiO_2 interface energy and the work of adhesion estimated using eqs 1 and 2 are given in Figure 4, where a negative interface energy at high temperatures is revealed.

The negative interface energies were reported for certain metal−metal systems, in which the heat of mixing was negative and interfacial alloying occurred through interdiffusion of metal atoms.[14,15] In general, the stronger the interactions between mixing components are, the more energy that is gained by forming the interface, and thus the more negative the interface energy would be.[16] For the Pt−SiO_2 system, the negative interface energy suggests a strong interactions between Pt and SiO_2. Since electron diffraction patterns shows no evidence of
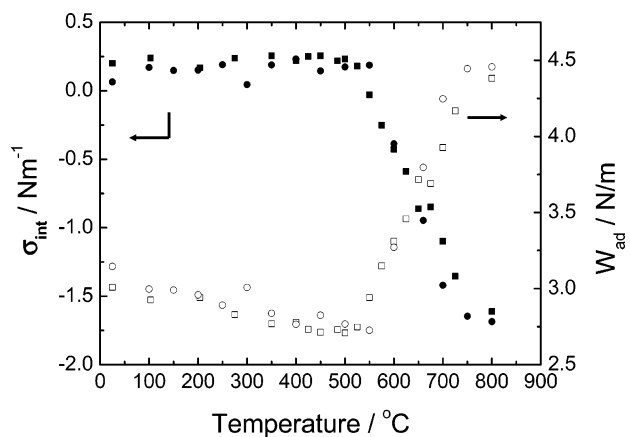
Figure 4. Interface energy and work of adhesion between Pt and SiO$_2$ at different temperatures. The squares and circles represent data from samples A and B, respectively.

alloying in Pt and SiO$_2$, the mixing could occur only at the Pt/SiO$_2$ interfaces.

There are several reports suggesting the strong Pt−SiO$_2$ interaction. By using X-ray photoelectron spectroscopy (XPS) and electron energy loss spectroscopy (EELS) studies, charge transfer was detected between Pt and SiO$_2$, resulting in a partial reduction of Si(IV).[17,18] Such an effect is much stronger for Pt than for other metals (Pd, Ag, and Au).[17] A high-energy ion beam was also shown to be able to induce the mixing of Pt films on the SiO$_2$ substrate, and the mixing is much more significant than that of Pt films on other substrates (Al$_2$O$_3$, SiC, and MgO).[19] In addition, the negative heat of interfacial mixing is expected to favor the surface diffusion of Pt on SiO$_2$ by Pt incorporation into the SiO$_2$ surface, consistent with the observation that the diffusion of Pt in SiO$_2$ was mainly through micropores or holes.[20,21]

Very recently, by employing grazing incidence small-angle X-ray scattering technique, it was observed that the horizontal size of Pt particles (about 3 nm in diameter) on an oxidized Si wafer increased above 320 °C.[22] The size increase was attributed to the agglomeration of the Pt particles.[22] Base on the present study, however, it is quite likely that the Pt particles spread on the substrate in this study as well. If true, it may suggest a size-effect of the wetting temperature.

Due to the negative interface energy, the work of adhesion between Pt and SiO$_2$ was large, as shown in Figure 4. The large work of adhesion implys that the detachment of the Pt particles would not take place at the Pt/SiO$_2$ interface but rather in the SiO$_2$ substrate. From the Griffith criterion,[23] the energy required for the fracture from the SiO$_2$ substrate is two times the SiO$_2$ surface energy (∼0.56 N/m), much less than the energy required for the fracture at the Pt/SiO$_2$ interface, i.e., the work of adhesion (∼3 N/m). Cordill et al. measured the adhesion of Pt films on the SiO$_2$ substrate using nanoindentation.[24] The fracture energy was calculated to be 0.2 and 0.5 N/m for indentation blisters and spontaneous buckles, respectively. The values are close to the present estimation (∼0.56 N/m) based on the Griffith criterion. In that work, however, the exact fracture position was not available.

In conclusion, the thermal stability of facetted Pt nanoparticles on silica support films has been investigated using in situ transmission electron microscopy. In addition to the shape changes, the particles' wettability on the support films increased with increasing temperature above a critical temperature of about 500 °C. Such thermal wetting of Pt nanoparticles on the silica surface suggests a negative interface energy between Pt and SiO$_2$ at high temperatures, which is attributed to the interfacial mixing of Pt and SiO$_2$. This insight could have important implications in elucidating the actual catalytic process for Pt/SiO$_2$ hetero-geneous catalysts, particularly at high temperature.

Supporting Information Available: Estimation of average contact angle from the projection area of the nanocrystals on silica grid. This material is available free of charge via the Internet at http://pubs.acs.org.

References and Notes

(1) Min, B. K.; Santra, A. K.; Goodman, D. W. *Catal. Today* **2003**, *85*, 113.

(2) Schubert, M. M.; Hackenberg, S.; van Veen, A. C.; Muhler, M.; Plzak, V.; Behm, R. J. *J. Catal.* **2001**, *197*, 113.

(3) Chen, M. S.; Goodman, D. W. *Science* **2004**, *306*, 252.

(4) Haruta, M. *Catal. Today* **1997**, *36*, 153.

(5) Wang, Z. L.; Petroski, J. M.; Green, T. C.; El-Sayed, M. A. *J. Phys. Chem. B* **1998**, *102*, 6145.

(6) Wang, D.; Penner, S.; Su, D. S.; Rupprechter, G.; Hayek, K.; Schlögl, R. *J. Catal.* **2003**, *219*, 434.

(7) Eppler, A. S.; Rupprechter, G.; Anderson, E. A.; Somorjai, G. A. *J. Phys. Chem. B* **2000**, *104*, 7286.

(8) Zhu J.; Somorjai, G. A. *Nano Lett.* **2004**, *1*, 8.

(9) Penner, S.; Wang, D.; Su, D. S.; Rupprechter, G.; Podloucky, R.; Schlögl, R.; Hayek, K. *Surf. Sci.* **2003**, *276*, 53.

(10) Bonzel, H. P. *Phys. Rep.* **2003**, *385*, 1.

(11) Murr, L. E. *Interfacial Phenomena in Metals and Alloys*; Addison-Wesley: Reading, PA, 1975.

(12) Song, H.; Kim, F.; Connor, S.; Somorjai, G. A.; Yang, P. *J. Phys. Chem. B* **2005**, *109*, 188.

(13) Brandes, E. A. *Smithells Metal Reference Book*, 6th ed.; Butterworth: London, 1983.

(14) Chan, C. T.; Bohnen, K. P.; Ho, K. M. *Phys. Rev. Lett.* **1992**, *69*, 1672.

(15) Rosset, S.; Chiang, S.; Fowler, D. E.; Chambliss, D. D. *Phys. Rev. Lett.* **1992**, *69*, 3200.

(16) Bauer, E. *Appl. Surf. Sci.* **1982**, *11/12*, 479.

(17) Komiyama, M.; Shimaguchi, T. *Surf. Interface Anal.* **2001**, *32*, 189.

(18) Klie, R. F.; Disko, M. M.; Browning, N. D. *J. Catal.* **2002**, *205*, 1.

(19) Nagel, R.; Balogh, A. G.; Behar, M. *Nucl. Instr. Methods B* **2002**, *187*, 459.

(20) Dallaporta, H.; Liehr, M.; Lewis, J. E. *Phys. Rev. B* **1990**, *41*, 5075.

(21) Liehr, M.; Dallaporta, H.; Lewis, J. E. *Appl. Phys. Lett.* **1988**, *53*, 589.

(22) Winans, R. E.; et al. *J. Phys. Chem. B* **2004**, *108*, 18105.

(23) Kelly, A.; Macmillan: N, H. *Strong Solids*, 3rd ed.; Clarendon Press: Oxford, U.K., 1986.

(24) Cordill, M. J.; Moody, N. R.; Bahr, D. F. *J. Mater. Res.* **2004**, *19*, 1818.